Third International Symposium on Marine Propulsors
smp'13, Launceston, Tasmania, Australia, May 2013

Propeller and Rudder in Off-Design Conditions

Thomas Lücke[1]

[1]Hamburgische Schiffbau-Versuchsanstalt GmbH (HSVA), Hamburg, Germany

ABSTRACT

As soon as a vessel does not operate in calm waters but under the influence of wind, waves and current, the vessel can drift and the operating conditions deviate from the so called (single) design point, normally obtained during the design stage. Under these circumstances the ship as well as propeller and manoeuvring devices will operate in off-design conditions for long term.

This paper summarizes the essential results of investigations done in this respect at HSVA for the national joint research project Off-Design (2012). By means of propulsion tests and wake measurements at straight course and under drift conditions some representative operating points were identified, defining the off-design conditions of a RoRo ferry. Propeller and rudder were then investigated in the cavitation tunnel in these conditions. Off-design propeller pitch settings were investigated as well.

By means of pressure pulse and cavitation inception test results the propeller characteristics are compared between straight course and drift conditions. Rudder force measurements show the consequences from the rudder point of view.

Keywords

off design, drift, cavitation, efficiency, CPP, cavitation inception

1 INTRODUCTION

When a ship and its propulsion plants as propellers and rudders are designed, the focus lays mainly on one design condition or contract point. While variations like draught changes are commonly considered during the design stage, unavoidable variations of the operating condition due to weather influences are much more difficult to be accounted for.

If the vessel is influenced by current or wind and waves related to weather conditions, the ship will drift with a certain drift angle β and the ship will operate in so called off-design conditions. From the propeller and rudder point of view their working environment is expected to change under these drift conditions. Focus is made on conditions which the ship will face for long term, i.e. relatively small drift angles and their influence onto efficiency and cavitation behavior.

2 INFLUENCE OF THE ENVIRONMENT ONTO THE OPERATING CONDITIONS

All the evaluations are based on model tests performed at HSVA. The ship model represents a RoRo ferry designed to operate in the North Sea between Netherland and Ireland. Its particulars are found in the appendix. The influence of the environmental condition onto the ship has been investigated at design draught with load varied propulsion tests under the Computerized Planar Motion Carriage (CPMC). Systematic variations of drift angles β (-10°,-4°,0°,4°,10°), propeller pitch angles ϕ (design pitch E, E-10.5°, E-5°), propeller speeds n, rudder angles δ and ship speeds Vs (13kts, 16kts, 19kts) have been investigated. The obtained results represent only possible ship reactions onto variable environmental conditions from the ship side of view. Only the combination with external forces due to imposed environmental conditions leads to the unique equilibrium condition of the ship represented by drift angle β, rudder angle δ and propeller revolutions n. The environmental conditions are defined by wind and wave loads depending on wind states BFT 0/3/6 at encounter angles ε between 0° and 360° (ε=0° headwind, 180° following wind).

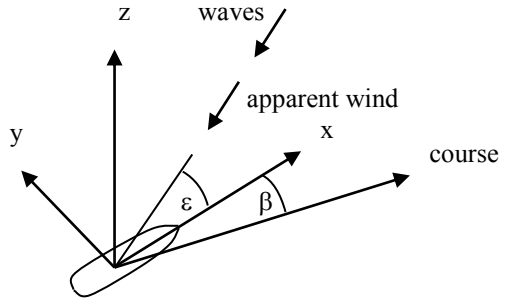

Figure 1: Sketch of drifting ship

For simplicity the apparent wind and the waves are assumed to encounter the ship at the same angle ε , see **Figure 1**. Wind and wave loads are imposed onto the ship by horizontal forces Fx, Fy and yawing moment Mz acc. to wind load coefficients Blendermann (1996) and acc. to strip method Söding (1994).

3 OFF-DESIGN CONDITIONS

Figure 2 shows exemplarily the environmental loads due to wind and waves versus encounter angle ε valid for 6BFT, where **Figure 3** shows the corresponding ship reactions β and δ. The highest drift and rudder angles are found at ε=±60°, whereas the highest power is needed at β=±30°. With lower ship speed the ship reacts more sensitive onto the environmental conditions. At constant environmental conditions higher rudder angles are necessary for course keeping at lower ship speeds compared to higher speeds. For example, rudder angles of 10°-13° are necessary to maintain drift angles of 3°- 4°. Typical rudder settings of δ=±5° during course keeping would suffice to maintain drift angles of β=1°-2°. **Table 1** compares operating conditions of 6BFT, ε=60° with the operating conditions at 0BFT (trial condition). To maintain ship speeds Vs=13kts/16kts/19kts under drift angles of about β=4°/3°/2°, the necessary propeller thrust increased by 72%, 42%, 27% and the delivered power PD increased by 60%, 49%, 30% in relation to BFT0.

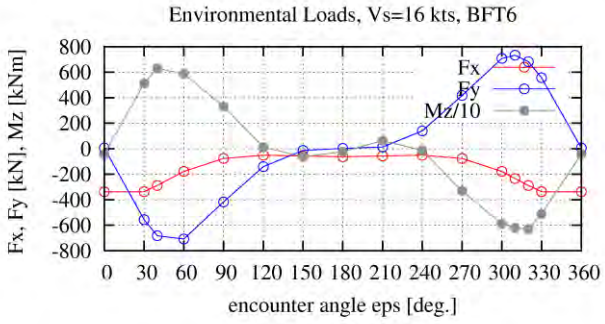

Figure 2: Environmental loads onto the ship at BFT6

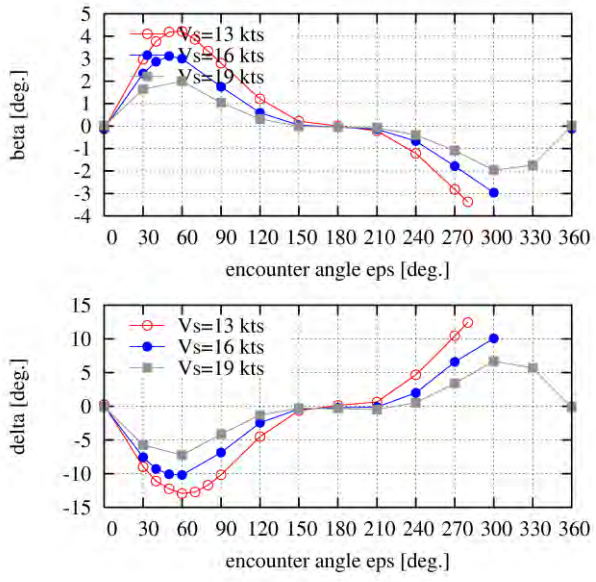

Figure 3: Drift- und rudder angles under steady drift courses at BFT6

Table 1: Operating points at trial condition (BFT0) versus drift condition (BFT6)

BFT 0			
	Vs=13kts	Vs=16kts	Vs=19kts
drift angle β	**0°**	**0°**	**0°**
rudder angle δ	0°	0°	0°
pitch	E-10.5°	E-5°	E
PD MCR[%]	35%	55%	86%
T [kN]	365	550	778
BFT 6, ε=60°			
drift angle β	**4.2°**	**3.0°**	**2.0°**
rudder angle δ	-13°	-10°	-7°
PD MCR[%]	56%	82%	112%
T [kN]	629	781	987
Difference between 6 BFT and 0 BFT			
ΔPD [%]	+60	+49	+30
ΔT [%]	+72	+42	+27

The above results point out, that many combinations are possible between environmental conditions and corresponding ship reactions. The variety of possible operating conditions should be reduced in order to be considered during the ship design. As an approach the minimal- and maximal values of delivered power PD have been presented as possible limit curves together with trial condition. As a consequence the detailed information of drift-, encounter- and rudder angles are omitted and only information like the increase in thrust, PD, n and propeller pitch keeps a matter of further consideration. **Figure 4** shows the results of such an approach. All curves have the mode of constant propeller speed in common. This operating mode is necessary in order to maintain the shaft frequency for the shaft generator (PTO). These curves show the delivered power consumption PD depending on weather conditions. The corresponding pitch settings (dϕ) in relation to design pitch ("E") are shown as well.

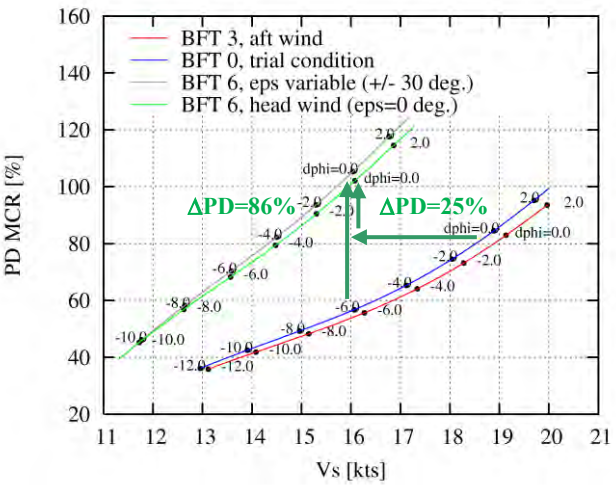

Figure 4: Propulsion behavior at off-design conditions (CPP), constant propeller speed

The power curves at low environment condition show the usual dependency PD~Vs^n, n>3 whereas at higher environmental conditions it changes to almost quadratic dependency PD~Vs^2.

Starting from the design point with design pitch (dφ=0°, Vs=19kts) on the trial curve (blue) it would be possible to operate at 6BFT under drift conditions (grey) with constant pitch in order to accept a decrease in ship speed and sail at about 16kts. As a consequence the delivered power increases by about 25%. Maintaining the speed of Vs=16kts (dφ = -6°) at 6BFT by increasing the pitch by dϕ=6° to design pitch (E), the power consumption increases by about 86%. The grey and green curves show the (small) amount of power difference between 6BFT headwind with and without drift and corresponding rudder settings. **Table 2** shows the limit values expected from the propeller point of view (pitch, thrust, power) compared to straight course (head wind and waves). Drift and corresponding rudder settings affect the power consumption depending on ship speed (compared to straight course). At low ship speed the power increased by about 1.6% whereas the thrust increased by 6%. At higher ship speed the power and thrust increased by 4% and 3% respectively. At BFT3 the weather conditions consist only of wind loads, since the predicted wave loads were too small to be reasonable considered. Especially following wind reduces relative wind speeds and lead to reduced propeller loading. Therefore the BFT3 curve valid for following wind (red) reflects the lowest possible limit curve. The decrease in propeller loading at the design point is about 2% in thrust and power. High following wind reduces the relative wind even further but the accompanied waves lead to higher resistance, see **Figure 2**, ε=180°.

Table 2: Reaction of propeller between straight course and drift condition

	BFT6, ε=0° straight course, head wind			
Vs [kn]	13	14	15	16
pitch dϕ [°]	-7.2	-5.1	-2.8	-0.2
PD MCR%	62	73	86	101
T [kN]	689	763	838	915
	BFT6, ε=+/-30°, drift			
pitch dϕ [°]	-7.2	-5.1	-2.8	-0.1
PD MCR%	63	76	89	105
T [kN]	732	798	869	944
	difference to straight course			
ΔPD [%]	1.6	4.0	3.5	4.0
ΔT [%]	6.0	4.6	3.7	3.2

4 INFLUENCE OF DIFFERENT PITCH SETTINGS AT STRAIGHT COURSE

Figure 5 shows the influence of pitch settings onto the delivered power versus ship speed at straight course. The propulsion tests have been performed with 3 pitch settings in the same speed range, where the evaluation has been done by interpolation in order to maintain a constant shaft frequency. Operating the propeller at fixed pitch but with variable propeller speed (blue curve), leads to the least power consumption. The red curve shows the power consumption when the vessel is operated at constant propeller speed but with varied propeller pitch. Both curves coincides near the design point (Vs=19kts, propeller pitch E, dϕ=0). Operating the ship at 14kts and reducing the pitch by 14° the delivered power increases by about 46% related to fixed pitch operation. The third curve (grey) depicts the power prognosis valid for the mode of constant propeller speed but with constant propulsion coefficients w, t, η_R, which are determined at design pitch. There are the wake fraction w, the thrust deduction fraction t and the relative rotative efficiency η_R. This grey curve reflects the information normally available during a design stage of a propeller, where only the stock propeller performance at one pitch setting is available. The difference to the red curve is surprisingly low, which encourage the pragmatic way to let the propulsion coefficients constant at first approximation in the design stage.

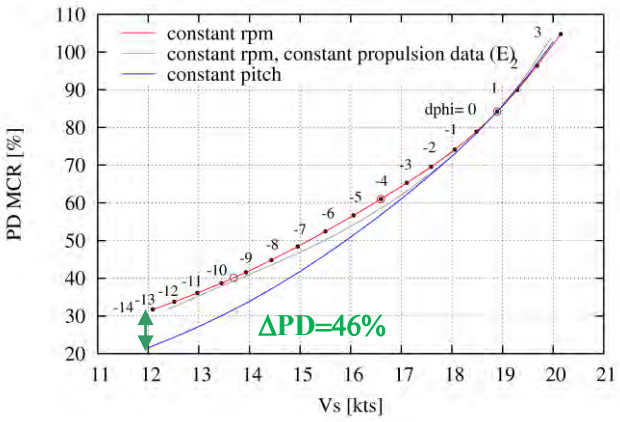

Figure 5: Power consumption at constant pitch versus constant propeller speed, trial condition

The major contribution to the increased power consumption at constant propeller speed is found in the reduced propeller efficiency η_0, see **Figure 6**. A minor part is found in the interaction between ship/rudder and the propeller in terms of η_H and η_R. Operating the propeller at constant pitch led to an increase of η_H with decreasing ship speed, whereas at constant propeller speed η_H kept constant. At medium pitch setting and ship speed the difference between red and grey curve derives from the η_R which is surprisingly low in relation to the lower and higher pitch settings.

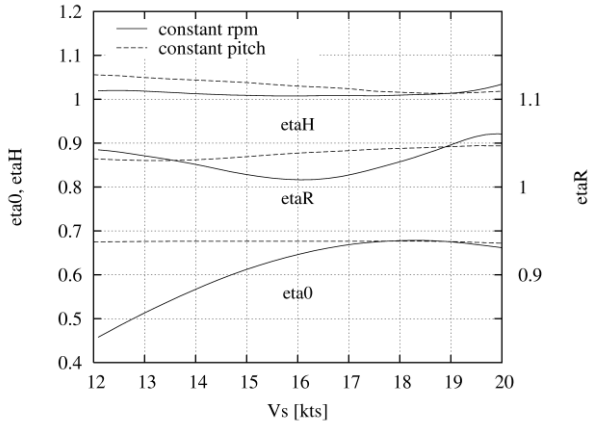

Figure 6: Efficiencies at constant pitch versus constant propeller speed, trial condition

If slow ship speeds in relation to the design speed are not frequently used then the relative high power consumption at constant propeller speed plays only a minor role. When the operating profile of this kind of ship is changed (slow steaming), the loss of efficiency will become more important.

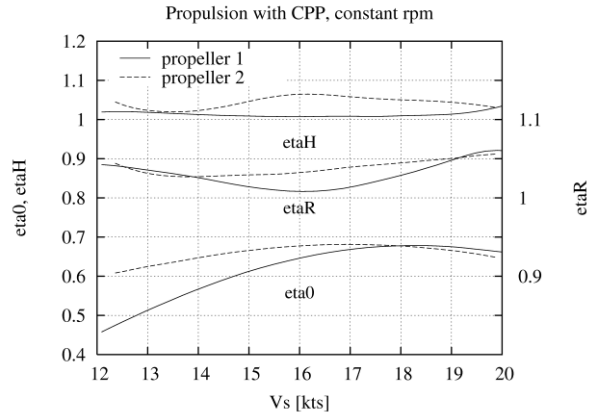

Figure 7: Efficiencies of two different propeller designs

Figure 7 shows the efficiencies of two different propeller designs. Propeller 1 is the original design, with cavitation pattern meeting the strong requirements of the customer. Propeller 2 was designed in order to delay face cavitation at low pitch and to increase the efficiency at lower speeds by accepting higher pressure pulses. The distribution of η_0 shows a maximum below the former design point (19kts) at about 16.5 kts. In the view of the mentioned slow steaming, the comparison shows, that a redesign could cope with the slower ship speeds to a certain amount. At reduced ship speed the pressure pulses are more or less equal and only above the original design speed, the pressure pulses and therefore the vibration induction is significantly increased, see **Figure 8**.

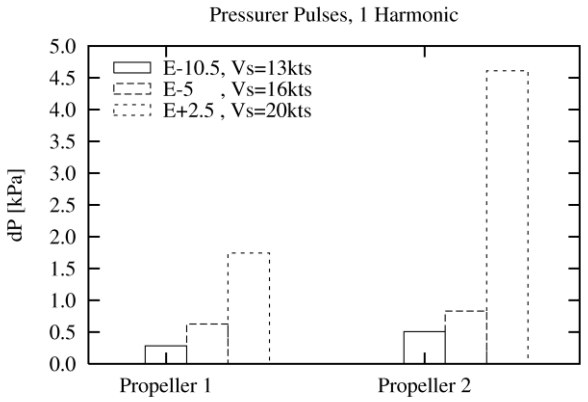

Figure 8: Pressure pulses of two different propeller designs

5 INFLUENCE OF THE OFF-DESIGN CONDITIONS ONTO PROPELLER AND RUDDER

5.1 Propeller

The influence of the different operating conditions onto the hydrodynamic characteristic of the propeller and rudder has been further investigated in the HYKAT, the largest cavitation tunnel of HSVA.

The ship model was installed into the HYKAT at drift angles β=–4°/0°/+4°. At all three drift angles the propeller pitch was kept constant to E-5° corresponding to Vs=16kts. At straight course off-design pitch settings of E-10.5° (Vs=13kts), E-5.0° (Vs=16kts) and E+2.5° (Vs=20kts) have been investigated as well.

When the propeller is operated at constant propeller speed, the lower ship speeds are realized by reduced pitch settings. Especially this pitch reduction decreases the onset of back cavitation but increases the onset of face cavitation, which normally should be avoided due to its possible danger of erosion.

Figure 9 shows the face cavitation inception diagram valid for straight course but with off-design pitch settings, where **Figure 10** shows the corresponding results for drift conditions at constant pitch E-5° (Vs=16kts). The cavitation diagrams represent cavitation number σ_n dependent on thrust coefficient KT.

$$\sigma_n = \frac{P - P_V}{\frac{\rho}{2}(\pi n D)^2} \quad (1)$$

$$K_T = \frac{T}{\rho n^2 D^4} \quad (2)$$

With static pressure at the point under consideration p, vapor pressure p_V, density of water ρ, diameter of propeller D and propeller thrust T. The intersection of the cavitation inception curves with the ship operating curve defines the cavitation inception speed (CIS) at $\sigma_{n,i}(K_{T,i})$. Operating points on the ship operating curve below the intersection point will lead to the cavitation pattern in question. The propeller showed vortex like face cavitation pattern, which needs to be scaled to full scale. At HSVA

this is done by scaling of the cavitation inception numbers acc. to McCormick (McCormick, 1962), (Friesch, 1995)

$$\sigma_{n,ship} = \sigma_{n,model} \left(\frac{Rn,ship}{Rn,model} \right)^{m} \qquad (3)$$

m=0.3

Figure 9 shows two almost vertical lines which represent ship operating curves at fixed pitches (E, E-5°) as well as the ship operating curve valid for constant propeller speed as horizontal line (σ_n=constant).

Cavitation inception curves are given for model scale (m=0) and full scale (m=0.3). Besides small differences, it is remarkable that the cavitation inception curves for three pitch settings coincide that way. In this particular case, the global unique trend (σ_n/K_T ~ constant) enforce a unique creating mechanism of the vortical face side cavitation pattern, which is created locally at the leading edge and almost independent of pitch. The reason for this can be found in the relatively high camber to pitch distribution, due to strong pressure pulse and vibration requirements. This high camber to pitch relation enforces the creation of a leading edge vortex during the periodic load decrease within the wake field.

For full scale, the cavitation inception speeds (CIS) could not be derived due to a lack of information, since the cavitation inception curves lay all above the ship operating curves without intersection point. The safety margin against the onset of face cavitation at design pitch was estimated at model scale to be -16% in KT (at constant σn). This result is depicted by the green arrow showing the distance in KT from the operating curve (E) to the inception curve at model scale. This safety margin is a usual and safe result for fixed pitch propellers. For a CPP especially with constant propeller speed this safety margin reduces significantly.

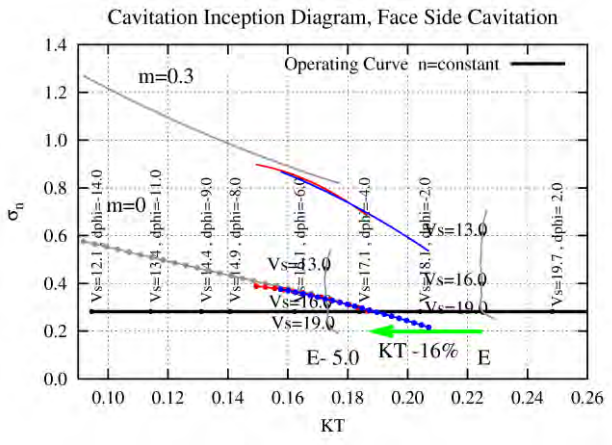

Figure 9: Face cavitation inception diagram, straight course

Under drift conditions the drift angle β enriches the cavitation inception diagram by one additional parameter. On the left hand side of **Figure 10** the ship operating curve for trial condition, BFT0 is shown together with the reference operating point Vs=16kts. Under influence of BFT3 and its related drift the KT varied by 4% (grey curve). The green curve represents the ship operating curve under the influence of drift for wind of BFT6 (0°≤ ε ≤ 360°). The operating curve covers a variation of 27% in KT and 32% in σ_n.

Since the CIS for full scale can"t be derived, a qualitative outlook onto the situation can be given even for model scale. The inception curves of the face cavitation valid for model scale at 3 drift angles are determined at β=-4°/0°/+4° and interpolated to match the operating conditions at constant pitch (E-5°, BFT6). The intersection points with the ship operating curve for BFT6 are marked by solid circles. The results show, that the face cavitation inception under drift conditions at BFT6 take place at Vs=16kts and about β= -1.8°/2.4°, whereas under straight course and the same environment condition the onset occurred already at Vs=19kts, E-5°.

Figure 11 shows the nominal wake field at straight course together with the blade position where face cavitation started to occure. **Figure 12** represents the wake field at drift angle β=4° (stern points to stb) showing almost the same velocity distribution on stb side and velocity defect on port side. For drift angle β=-4° however the wake field would show a distribution mirrored at the center line. Instead of mirroring the wake field, the sense of propeller rotation is changed graphically from left handed to right handed. The corresponding blade position of occurring face cavitation at β=-4° is shown in the **Figure 12** as well. Only the lee side leads to significant changes in the flow field, i.e. reduced axial component, with corresponding changes in cavitation inception.

Figures 13 and **14** show the comparison of the piecewise pressure signals for one single propeller revolution and corresponding FFT-spectra valid for the same KT and pitch but for different drift angles (E-5°, Vs=16kts). Almost no cavitation occurred at this reduced speed and pitch setting. At β=-4° (stern points to port side) the time signal shows high frequent oscillations in relation to the other drift angles. The source of this pattern is the earlier back side cavitation inception and its corresponding higher cavitation volume variation. With increasing drift angle (β=0°, 4°), where the stern points to stb, the oscillations diminish. Here the influence of back cavitation is visible, which increases at drift angle β=-4°. As a consequence the FFT spectrum at β=-4° shows increased amplitudes above the 2nd harmonic related to the other drift angles.

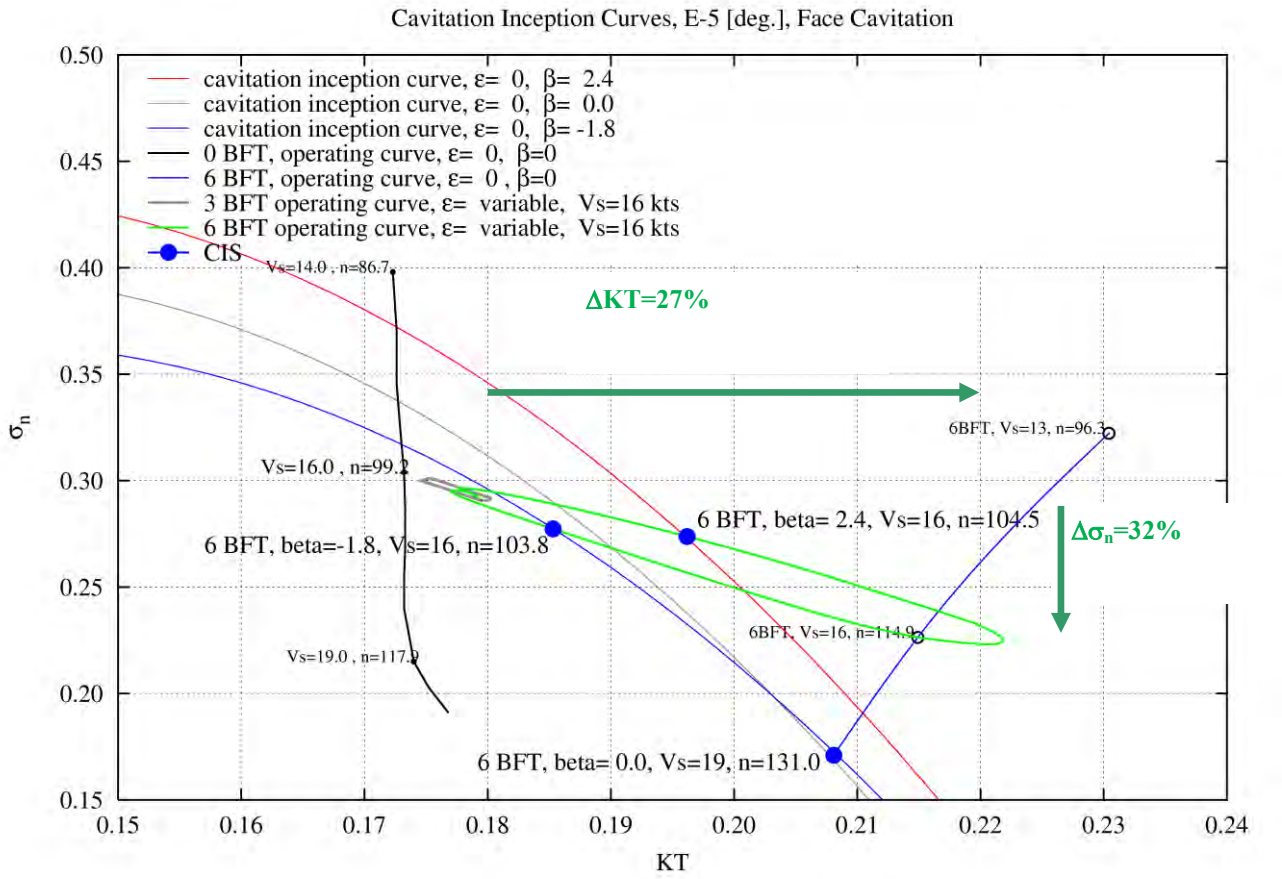

Figure 10: Face cavitation inception diagram, drift courses

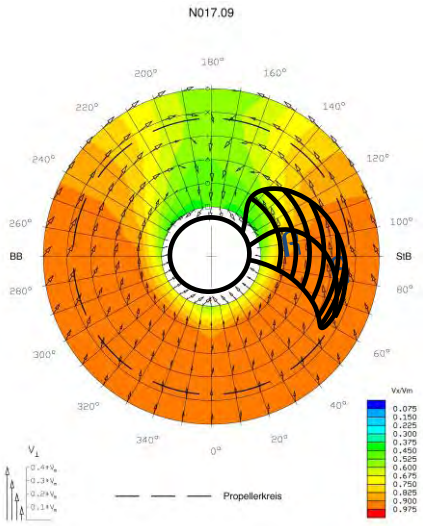

Figure 11: Influence of drift onto wake field and cavitation inception, β=0°

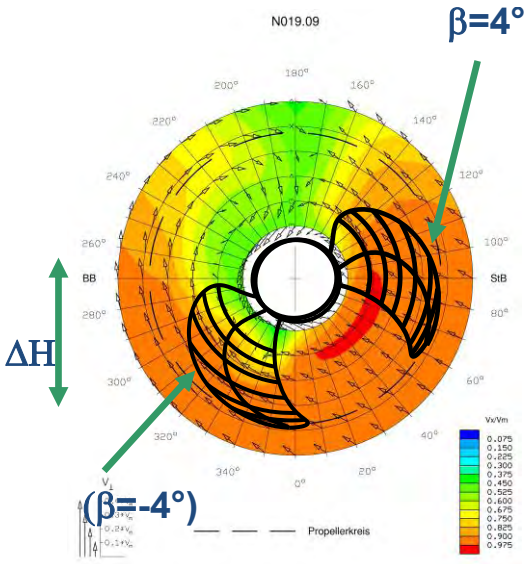

Figure 12: Influence of drift onto wake field and cavitation inception, β=-4° and +4°

At least this particular example shows only a drawback effect of drift onto the back side cavitation and its influence onto earlier cavitation inception and pressure pulses radiated form the propeller. Considering that this effect is further increased at lower speeds and therefore higher drift angles, the cavitation and its pressure pulses are expected not to cause any problems in relation to straight course. Even for face side cavitation the increased mean propeller load and the decreased local axial flow component on the lee side of the drifting ship lead to the fact that this particular point of face cavitation looses significance under drift conditions.

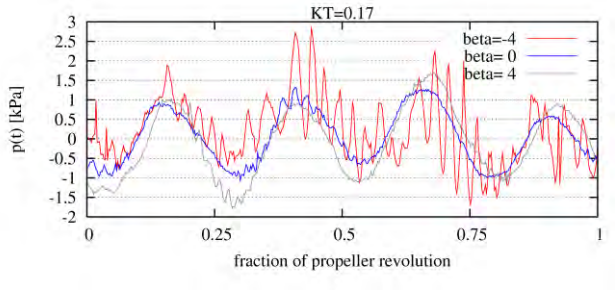

Figure 13: Pressure signals under drift conditions

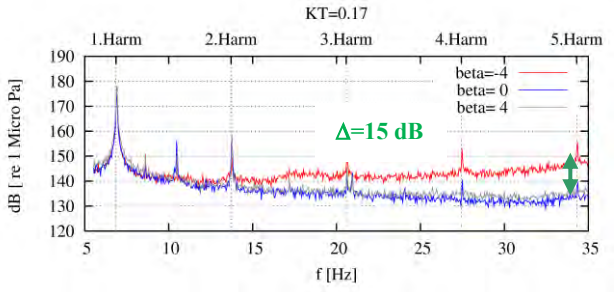

Figure 14: FFT Spectra under drift conditions

5.2 Rudder

Rudder force measurements were performed between rudder angles δ -45° and 45° in steps of 4° and 2° near the neutral rudder position and the stall angle. The ship model was fixed into the HYKAT, therefore the influence of the turning ship onto the rudder reactions is not accounted for. The rudder represents a full spade rudder with rudder bulb and with twisted profiles. During these measurements focus was set to ship fixed rudder reactions Fx in ship longitudinal direction (pos to bow) and Fy in transvers direction (pos. to port). The ship fixed rudder reactions Fx, Fy have been transformed into rudder fixed reactions lift L and drag D. These values, which are valid for model scale, have been normalized into coefficients CL and CD. Basis of the normalization are the density of the tunnel water ρ_{Tunnel}=0.9984 t/m^3, (t=18.5°C) the lateral area of the rudder S=cm*h=0.03205m^2, the height of the rudder h=0.221m, the mean profile length cm=0.145m and the mean axial velocity Va including the mean value of the induced axial velocity dV within the propeller slip stream (Brix, 1993). The induced velocity accounts the factor km, which refers to the distance dx between propeller plane and rudder axis dx=1.14*R, R = propeller radius.

$$L = -Fx \cdot \sin(\delta) + Fy \cdot \cos(\delta) \quad [\text{N}] \quad (4)$$

$$D = -Fx \cdot \cos(\delta) - Fy \cdot \sin(\delta) \quad [\text{N}] \quad (5)$$

$$CL = \frac{L}{\frac{\rho_{Tunnel}}{2} \cdot Va^2 \cdot S} \quad (6)$$

$$CD = \frac{D}{\frac{\rho_{Tunnel}}{2} \cdot Va^2 \cdot S} \quad (7)$$

$$Va = U_0 \cdot (1 - w) + dV \quad [\text{m/s}] \quad (8)$$

$$dV = U_0 \cdot km \cdot (-1 + \sqrt{1 + CTH}) \quad [\text{m/s}] \quad (9)$$

with km = 0.9

The results for constant ship speed Vs=16kts and variable drift angles β=-4°/0°/+4° are shown in **Figure 15**, whereas for straight course but different propeller pitch settings and corresponding ship speeds the results are shown in **Figure 16**.

The distribution of CL and CD versus rudder angle δ is almost symmetrical (CD) or point-symmetrical (CL) respectively to the neutral rudder angle. The stall angle is similar independent on propeller pitch or drift angle, only the rudder angle (pos./neg.) and therefore the location of the rudders suction side (ps/stb) shows an influence onto the stall angle.

At small rudder angles the rudder shows almost the same CD distribution but a parallel shift in the CL distribution. The shift amounts to -4° and +2° for -4° and +4° drift angle. Therefore this shift reflects the drift only to some extent. Due to the normalization of L and D dominantly by velocity Va^2, the pitch and corresponding speed variation lead to similar coefficients CD and CL for each pitch, see **Figure 16**. The different transvers component of the propeller swirl depending on propeller pitch and the related angle of attack for the rudder was expected to have a higher influence onto the rudder reactions.

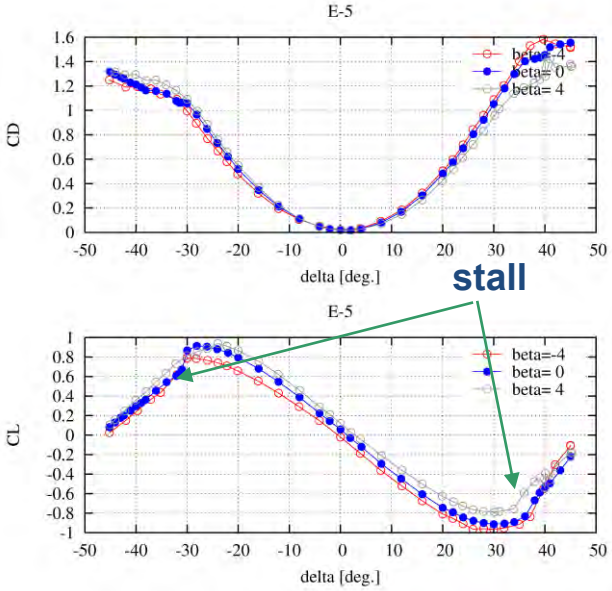

Figure 15: Influence of drift onto rudder forces

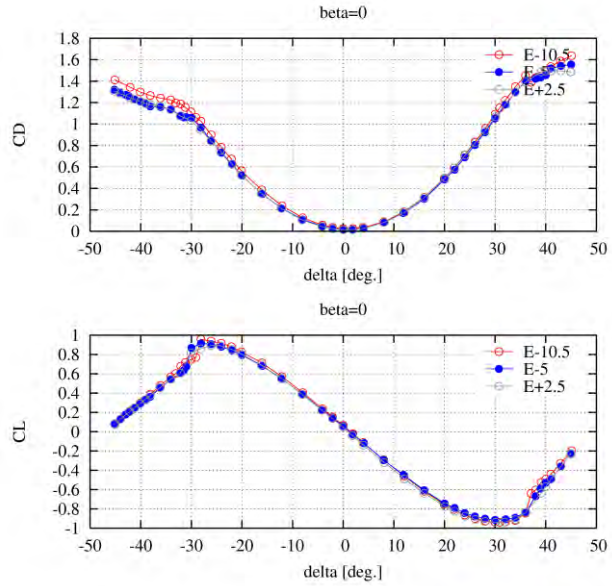

Figure 16: Influence of propeller pitch onto rudder forces

6 CONCLUSION

By means of propulsion tests at straight course and under drift conditions some representative operating points were identified, defining the off-design conditions of a RoRo ferry. Propeller and rudder were then investigated in the cavitation tunnel in these conditions. Off-design propeller pitch settings were investigated as well.

The main results can be summarized as follows:

- With reduced ship speed the ship reacts more sensitive onto weather conditions. At constant weather condition higher rudder angles were necessary for course keeping at reduced ship speed compared to higher ship speed. Significant drift angles of 3° - 4° correspond to rudder angles of 10° - 13°.
- To maintain 16kts ship speed with constant propeller speed and variable propeller pitch the power consumption increased by 86% under drift conditions at 6BFT compared to trial conditions.
- The propeller thrust due to drift and corresponding rudder angles increased compared to straight course at the same weather conditions up to 6%.
- Under drift conditions back cavitation started earlier and showed more pronounced cavitation pattern than at straight course. The highest drift angles occurred at lowest investigated ship speed and propeller pitch. Due to the corresponding low extent of sheet cavitation the propeller induced vibration induction of the ship will be low.
- The danger of occurring face cavitation under drift conditions is lower than under straight course, since these drift conditions require higher thrust and pitch, which delay the face cavitation inception.
- Under straight course at trial condition the danger of occurring face cavitation increases significantly with decreasing ship speed and corresponding decreasing propeller pitch. Further the power consumption increases as well with decreasing pitch in relation to constant propeller pitch operation (46%). The major contribution to the increased power consumption at constant propeller speed is found in the reduced propeller efficiency η_0, rather than in the interaction between ship/rudder and the propeller in terms of η_H and η_R.

7 ACKNOWLEDGEMENT

The referenced work has been supported by the national joint research project “Off-Design”, with the following partners: Flensburger Schiffbau-Gesellschaft mbH & Co. KG (FSG), Technische Univerität Hamburg Harburg (TUHH) and Energie-Umwelt-Beratung e.V (EUB).

8 REFERENCES

Lücke, T. (2012). „Off-Design – Entwicklung und Verifizierung hydrodynamisvher Berechnungs-methoden für Propulsions- und Manöverorgane im Off-Design“, HSVA-Report 1671 (K03-12), Hamburgische Schiffbau-Versuchsanstalt GmbH

Blendermann, W, (1996). „Wind Loading of Ships – Collected Data From Wind Tunnel Tests in Uniform Flow“, Report 574, Institut für Schiffbau der Universität Hamburg

Söding, H. (1994). Description of Program STRIP

Friesch, J., Johannsen, C., (1995). „Study on Tip Vortex Cavitation Inception for Navy Propellers“, International Symposium on Cavitation, Deauville, 2-5 May

McCormick, B.W. (1962). „On Cavitation Produced by a Vortex Trailing from a Lifting Surface", Journal of Basic Engineering

Brix, J. (1993) : „Manoeuvering Technical Manual", Seehafen Verlag

9 APPENDIX

The main particulars of the RoRo ferry are found in the table below.

Length between perpendiculars	186.220 m
Length at waterline	190.220 m
Breadth at waterline	26.200 m
Design draught	7.050m
Displacement	21329.9 m^3
Block coefficient	0.6201
Centre of buoyancy from AP	86.539 m
Model scale	24.829
Moveable rudder area	19.755 m^2
Aspect ratio (height/profile length)	1.524
Propeller diameter	5.8m
Propeller mean pitch ratio	1.08350
Hub diameter ratio	0.27700
Area ratio	0.65490
Number of blades	4
Sense of rotation	left
Propeller type	CPP